Comparative Study of the Morphology, Aggregation, Adherence to Glass, and Surface-Enhanced Raman Scattering Activity of Silver Nanoparticles Prepared by Chemical Reduction of Ag +...

ARTICLE *in* LANGMUIR · SEPTEMBER 2005

Impact Factor: 4.46 · DOI: 10.1021/la050030l · Source: PubMed

Comparative Study of the Morphology, Aggregation, Adherence to Glass, and Surface-Enhanced Raman Scattering Activity of Silver Nanoparticles Prepared by Chemical Reduction of Ag^+ Using Citrate and Hydroxylamine

M. V. Cañamares,[†] J. V. Garcia-Ramos,[†] J. D. Gómez-Varga,[‡] C. Domingo,[†] and S. Sanchez-Cortes*,[†]

Instituto de Estructura de la Materia, CSIC, Serrano 121, and Instituto de Ciencia y Tecnología de Polímeros, CSIC, Juan de la Cierva 3, 28006-Madrid, Spain

Received January 5, 2005. In Final Form: June 13, 2005

Two different silver colloids were prepared by chemical reduction of silver nitrate with trisodium citrate and hydroxylamine hydrochloride to compare their characteristics in relation to their possible use in surface-enhanced Raman scattering (SERS) spectroscopy. The morphology and plasmon resonance of the single nanoparticles and aggregates integrating these colloids were characterized by means of UV−vis absorption spectroscopy and scanning electron microscopy, revealing important differences between each type of nanoparticle as concerns their physical properties. These metallic systems also manifested differences in the aggregation and the adherence to glass surfaces, revealing significant differences in the chemical surface properties of these nanoparticles. SERS and surface-enhanced IR also indicated the presence of interference bands which can overlap the spectra of the analyte, mainly in the case of the citrate colloid. All these differences have an important influence on the applicability of these nanostructured systems in SERS. In fact, the enhancement factor and spectral pattern of the SERS obtained by using alizarin as a molecule probe are different.

Introduction

Surface-enhanced Raman scattering (SERS) represented a great advance in the field of Raman spectroscopy during the 1970s since the inherent weakness of the Raman signal can be substantially increased by 6 or more orders of magnitude. SERS is based on the huge enhancement of Raman emission of certain molecules when they are placed in the proximities of certain rough metal surfaces.[1,2] This technique can be successfully applied in the study of poorly soluble compounds in water, since very low concentrations are required, with the additional advantage of the fluorescence quenching occurring on the metal surface.[3,4]

The use of SERS in analytical studies strongly depends on the optical and electrical characteristics of the nanostructured metal employed as substrate. During the past few decades many different methods have been proposed in the preparation of metal nanostructured substrates valid for SERS.[5−16] Among these substrates, colloidal nanoscale particles have been the most frequently used. Metal colloids, in particular Ag and Au, were first used as substrates in SERS by Creighton et al.[5] Among the possible metals with applications in SERS (Ag, Au, and Cu), silver is the more universal substrate for several reasons: broad plasmon resonance in the visible−near-infrared region, high stability, and easy preparation. There are several methods to prepare Ag metal colloids employed in SERS: chemical reduction, photoinduced reduction,[17] or laser ablation.[18]

The preparation of Ag colloids in suspension by chemical reduction is a universally used method for SERS experiments. It is usually performed by using as the starting Ag salt silver nitrate, which is reduced by a chemical reducing agent to produce colloidal suspensions integrated by nanoparticles with variable size depending on the method (generally between 10 and 80 nm). The most frequently used reducing agents are trisodium citrate[7,19] and sodium borohydride.[5] In general, the use of a chemical reducing agent has the advantage of the feasibility and rapid preparation of the colloidal suspension together with the higher stability of the suspended nanoparticles. This

* To whom correspondence should be addressed. Fax: +34 91 5 64 55 57. Phone: +34 91 5 61 68 00. E-mail: imts158@iem.cfmac.csic.es.

† Instituto de Estructura de la Materia.

‡ Instituto de Ciencia y Tecnología de Polímeros.

(1) Moskovits, M. *Rev. Mod. Phys*. **1985**, *57*, 783.
(2) Wokaun, A. *Mol. Phys.* **1985**, *56*, 1.
(3) Hildebrandt, P.; Stockburger, M. *J. Phys. Chem.* **1984**, *88*, 5935.
(4) Jancura, D.; Sanchez-Cortes, S.; Kocisova, E.; Miskovsky, P.; Tinti, A.; Bertoluzza, A. *Biospectroscopy* **1995**, *1*, 265.
(5) Creighton, J. A.; Blatchford, C. G.; Albrecht, M. G. *J. Chem. Soc., Faraday Trans. 2* **1979**, *75*, 790.
(6) Sapieszko, R. S.; Matijevic, E. *J. Colloid Interface Sci.* **1980**, *74*, 405.
(7) Lee, P. C.; Meisel, D. *J. Phys. Chem.* **1982**, *86*, 3391.
(8) Ni, F.; Cotton, T. M. *Anal. Chem.* **1986**, *58*, 3159.
(9) Curtis, A. C.; Duff, D. G.; Edwards, P. P.; Jefferson, D. A.; Johnson, B. F. G:; Kirkland, A. I.; Wallace, A. S. *J. Phys. Chem.* **1988**, *92*, 2270.
(10) Akbarian, F.; Dunn, B. S.; Zink, J, I. *J. Phys. Chem.* **1995**, *99*, 3892.
(11) Tarcha, P. J.; DeSaja-Gonzalez, J.; Rodríguez-Llorente, S.; Aroca, R. *Appl. Spectrosc.* **1999**, *53*, 43.
(12) Shipway, A. N.; Katz, E.; Willner, I. *ChemPhysChem* **2000**, *1*, 18.
(13) Haynes, C. L.; Van Duyne, R. P. *J. Phys. Chem.* **2001**, *105*, 5599.
(14) Rivas, L.; Sanchez-Cortes, S.; García-Ramos, J. V.; Morcillo, G. *Langmuir* **2001**, *17*, 574.
(15) Hu, J.; Zhao, B.; Xu, W.; Fan, Y.; Li, B.; Ozaki, Y. *Langmuir* **2002**, *18*, 6839.
(16) Wang, Z.; Pan, S.; Krauss, T. D.; Du, H.; Rothberg, L. J. *Proc. Natl. Acad. Sci. U.S.A.* **2003**, *100*, 8638.
(17) Muniz-Miranda, M. *J. Raman Spectrosc*. **2004**, *35*, 839.
(18) Neddersen, J.; Chumanov, G.; Cotton, T. M. *Appl. Spectrosc.* **1993**, *47*, 1959.
(19) Sutherland, W. S.; Winefordner, J. D., *J. Colloid Interface Sci.* **1984**, *99*, 270.

10.1021/la050030l CCC: $30.25
Published on Web 07/29/2005

stability is due to the adsorption of the counterions of the salts employed in the colloid preparation, which confers a high electric charge to the nanoparticles. However, these colloids display several disadvantages such as the existence of impurities resulting from the oxidation residual species and the counterions of the employed salts.[20,21]

Recently, other chemical reducing agents have been used such as hydrazine[22] or hydroxylamine,[23] with the advantages of an easier preparation, since the reduction reaction can be done at room temperature, and the elimination of the residual oxidation products, which are, in the case of hydroxylamine colloid molecular nitrogen and nitrogen oxides.

Despite the higher stability of the chemically prepared Ag colloids, a partial aggregation is necessary for them to become active in SERS.[24] This aggregation leads to less stable systems with limited use in time. A possible solution to such a problem is the immobilization of the nanoparticles onto substrates. This can be accomplished by a direct procedure[25] or by a previous functionalization of the surface.[26]

The method employed in the preparation of metal colloids is an important factor to take into account in SERS, since it determines the morphology and the chemicophysical properties of the obtained nanostructured metal surfaces, which are also related to their aggregation and immobilization ability. However, less attention has been devoted so far to the study of the influence of the preparation method to all these properties and the comparison between different preparation methodologies.

In this paper we report a comparative study of the physicochemical properties of Ag nanoparticles prepared by a classic method, i.e., by using as the chemical reducing agent trisodium citrate and Ag nanoparticles prepared by means of hydroxylamine. In this study we have employed scanning electron microscopy (SEM), UV−vis absorption, SERS, and surface-enhanced IR (SEIR) spectroscopy to investigate the morphology, aggregation, adherence onto a glass surface, impurity content, and SERS effectiveness of the prepared nanoparticles. To check the SERS activity of the above-mentioned colloids, we have used alizarine (1,2-dihydroxyanthraquinone, AZ) as a molecular probe. This molecule was characterized by SERS spectroscopy in a previous work.[27]

Experimental Section

Materials. $AgNO_3$, trisodium citrate, and hydroxylamine hydrochloride were purchased from Sigma. AZ was purchased from Acros (97%). Stock solutions of the dye were prepared in a 0.1 M sodium hydroxide solution. The last solution was further diluted in water to a final concentration of 10^{-2} M. All the reagents employed were of analytical grade and purchased from Sigma and Merck. The aqueous solutions were prepared by using triply distilled water.

Preparation of Ag Colloids. Silver colloids were prepared by reduction of silver nitrate with two different reduction agents: trisodium citrate dihydrate and hydroxylamine hydrochloride.

Ag−Citrate (SC) Colloid. The SC colloid was obtained according to the method described by Lee and Meisel.[7] A total of 1 mL of a 1% w/v trisodium citrate aqueous solution was added to 50 mL of a boiling 10^{-3} M silver nitrate aqueous solution, and boiling was continued for 1 h. The colloid obtained showed a turbid gray aspect and had a final pH of 6.5.

Ag−Hydroxylamine (SH) Colloid. The SH colloid was obtained by the method described by Leopold and Lendl.[23] A total of 4.5 mL of a sodium hydroxide solution (0.1 M) was added to 5 mL of a 6×10^{-2} M hydroxylamine hydrochloride solution. Then the mixture was added rapidly to 90 mL of a 1.11×10^{-3} M silver nitrate aqueous solution, and the resulting mixture was shaken until a homogeneous mixture was obtained. The resulting colloid showed a milky gray color. The stability of the colloid prepared in this way was lower than that of the SC colloid, due to the formation of nitrogen oxides as a consequence of the reduction process of silver nitrate. Because of the reaction of these oxides with water, the pH of the Ag−hydroxylamine colloids tends to slightly decrease with time. Therefore, aqueous NaOH was added to the final solution to bring the pH to 6.5.

Aggregation of Silver Nanoparticles. The colloids were aggregated by addition of potassium nitrate so they would become active in SERS.[28,29] The activation was performed by adding 20 μL of a 0.5 M potassium nitrate solution to 500 μL of both SC and SH colloids. This activation method gives rise to a homogeneous aggregation of Ag nanoparticles as demonstrated by the SEM micrographs.

Immobilization of Ag Nanoparticles and Nanoaggregates. Unaggregated Ag nanoparticles or nanoaggregates (obtained after aggregation of Ag nanoparticles) were immobilized by direct deposition of 20 μL of the particle suspension on a glass cover slide. Then the solvent was allowed to evaporate at room temperature. The dried drop was then washed with tridistilled water several times to remove any salt residue.

Preparation of Samples for SERS and SEIR Experiments. Samples for macro-SERS experiments of blank colloids (in the absence of AZ) were prepared as described above by adding nitrate. Samples for SERS of AZ were prepared by adding 5 μL of the dye aqueous solution described above to 500 μL of the already aggregated colloid (after addition of nitrate). In all cases the colloidal suspension was placed in a quartz cuvette.

Samples for micro-SERS experiments of blank colloids (in the absence of adsorbate) were prepared by placing an aliquot of the original nonactivated colloid on a glass slide provided with a shallow groove (2 cm diameter and 0.38 mm depth). Then the cover glass slide with the immobilized Ag nanoparticle film, obtained according to the procedure described above, was placed on the groove with the side containing the nanoparticles facing downward in contact with the suspension placed in the groove.

Samples for SEIR experiments were prepared in transmission mode by placing an aliquot of the original nonactivated colloid on CaF_2 (the SC colloid) and on Ge (the SH colloid) slides. Ge was employed in the case of SH colloids to investigate the possible presence of nitrogen oxides in the sample, since this material transmits IR light to a lower wavenumber than CaF_2. The dried drop was analyzed before and after washing with tridistilled water several times to remove the excess nitrate.

Preparation of Samples for UV−Vis Absorption Spectroscopy. Samples for UV−vis spectroscopy of the colloids were prepared by solving 300 μL of the colloid in 3 mL of water. Quartz cells of 1 cm optical path length were used.

Preparation of Samples for SEM. The samples obtained by immobilization of nanoaggregates on a glass cover slide were also employed for SEM observation. All samples were coated at room temperature with a 3−4 nm gold/palladium (Au/Pd) layer using a high-resolution magnetron sputter coater operated at 800 V and a 5 mA plasma current to get a coating rate of 0.5 nm/min.

Instrumentation. The SERS spectra were recorded in a Renishaw RM2000 micro-Raman instrument. The 785 nm excitation line used was provided by a diode laser. The samples

(20) Munro, C. H.; Smith, W. E.; Garner, M.; Clarkson, J.; White, P. C. *Langmuir* **1995**, *11*, 3712.
(21) Sanchez-Cortes, S.; García-Ramos, J. V. *J. Raman Spectrosc.* **1998**, *29*, 365.
(22) Nickel, U.; Mansyreff, K.; Schneider, S. *J. Raman Spectrosc.* **2004**, *35*, 101.
(23) Leopold, N.; Lendl, B. *J. Phys. Chem. B* **2003**, *107*, 5723.
(24) Blatchford, C. G.; Campbell, J. R:; Creighton, J. A. *Surf. Sci.* **1982**, *120*, 435.
(25) Bjerneld, E. J.; Johansson, P.; Käll, M. *Single Mol.* **2000**, *1*, 239.
(26) Chumanov, G.; Sokolov, K.; Gregory, B. W.; Cotton, T. M. *J. Phys. Chem.* **1995**, *99*, 9466.
(27) Cañamares, M. V., Sánchez-Cortés, S., Domingo, C.; García Ramos, J. V. *J. Raman Spectrosc.* **2004**, *35*, 921.
(28) Sanchez-Cortes, S., Garcia-Ramos, J. V.; Morcillo, G. *J. Colloid Interface Sci.* **1994**, *167*, 428.
(29) Sanchez-Cortes, S., Garcia-Ramos, J. V., Morcillo, G.; Tinti, A. *J. Colloid Interface Sci.* **1995**, *175*, 358.

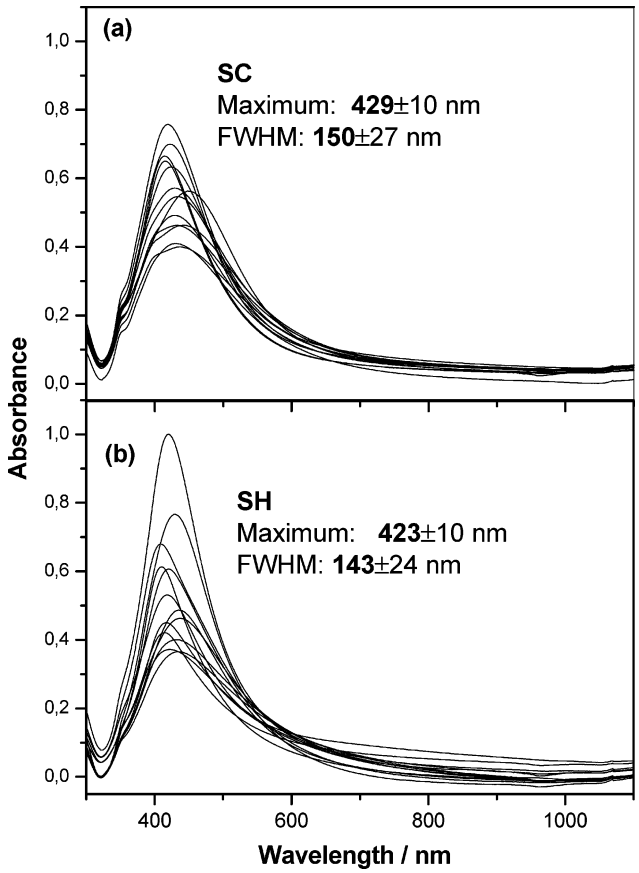

Figure 1. UV absorption spectra of different SC (a) and SH (b) colloid preparations.

were measured in a quartz cell of 1 cm optical path length placed in a macrosampling accessory with a focalization lens of 15 mm. The laser power at the sample was 2 mW. The resolution was set at 4 cm^{-1}, and the geometry of micro-Raman measurements was 180°.

FT-Raman and SERS spectra were obtained by using an RFS 100/S Bruker spectrometer. The 1064 nm line, provided by a Nd:YAG laser, was used as the excitation line. The resolution was set to 4 cm^{-1}, and a 180° geometry was employed. The output laser power was 150 mW.

The SEIR spectra were measured on an FTIR Bruker IFS 66 spectrometer provided with a DTGS detector. The spectral resolution was 8 cm^{-1}, and 100 scans were obtained from each sample.

UV−vis absorption spectra were recorded with a Cintra 5 spectrometer. The samples were put in 1 cm optical path length cuvettes.

SEM micrographs were taken in an environmental scanning electron microscope, PHILIPS XL30, with a tungsten filament operating in high-vacuum mode. The acceleration voltage was 25 kV. For secondary electrons, the standard Everhart−Thornley detector was used.

Sample coating was accomplished using a high-resolution magnetron sputter coater, Polaron SC 7640.

Results and Discussion

UV−Vis Spectroscopy and SEM. *Unaggregated Ag Colloids*. Figure 1 shows the UV−vis absorption spectra of SC (Figure 1a) and SH (Figure 1b) colloids corresponding to 13 different batches prepared on different days. The average plasmon absorption maximum, absorbance at the maximum, and full width at half-maximum (fwhm) are indicated in the corresponding panel for each colloid.

It is worth noting that the absorption spectrum changes from batch to batch, and this could have importance in quantitative analytical detections. This demonstrates that small modifications in the nanoparticle preparation have dramatic effects on the resulting suspensions as also revealed by other authors.[23,30] Even so, there are general differences between these two colloids: the maximum is significantly shifted upward in the case of the SC colloid (429 nm) with respect to that of the SH colloid (at 423 nm), at a confidence level of ca. 90%. The absorption broadness is also higher in the case of the SC colloid, and the corresponding standard deviations of the maximum and fwhm are higher in the case of the SC colloid, while the SH colloid displays a much higher standard deviation in the absorption value at the maximum.

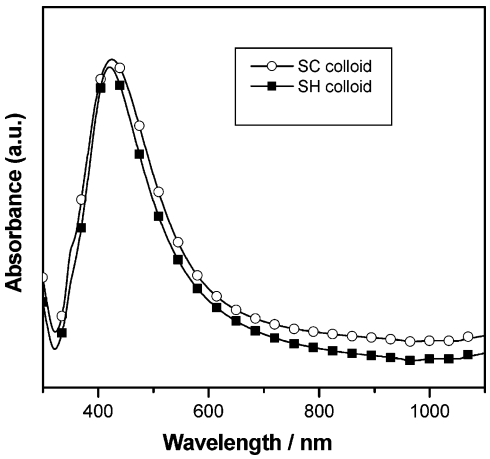

Figure 2. Average UV−vis absorption spectra of the SC (○) and SH (■) colloid spectra shown in Figure 1.

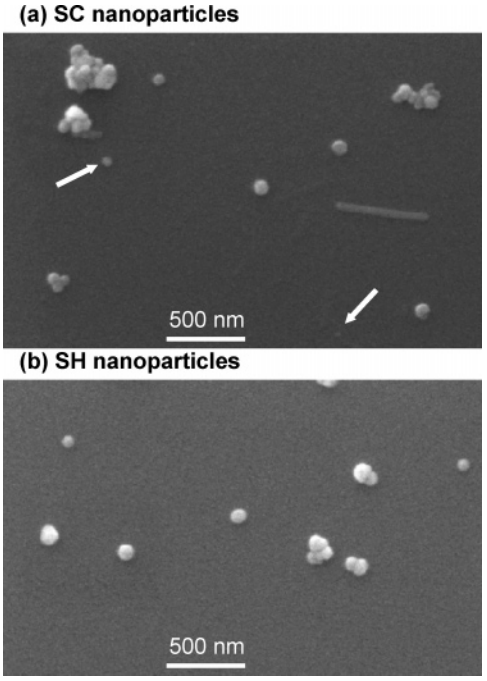

Figure 3. SEM micrographs of SC (a) and SH (b) nonaggregated nanoparticles.

Figure 2 shows the average SC and SH UV−vis absorption spectra, also reflecting the broader plasmon absorption of the SC colloid, and the slight shift of the absorption maximum toward higher wavelength values.

Figure 3 displays the SEM micrographs for the nonaggregated SC (Figure 3a) and SH (Figure 3b) colloids immobilized on a glass surface. The SC colloid shows a

(30) Cook, J. C.; Cuypers, C. M. P.; Kip, B. J.; Meier, R.; Koglin, E. *J. Raman Spectrosc.* **1993**, *24*, 609.

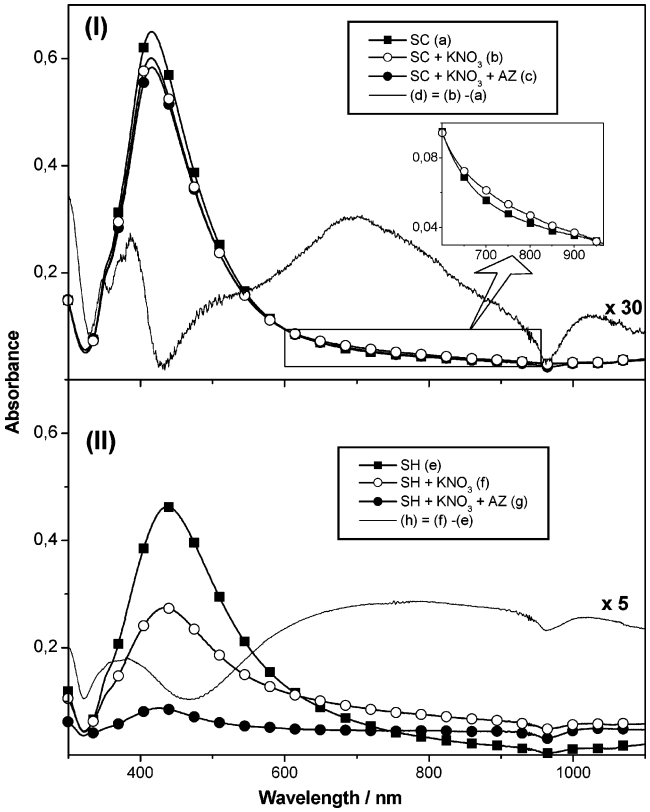

Figure 4. UV−vis absorption spectra of (I) the SC colloid [(a) nonaggregated colloid, (b) aggregated colloid with KNO_3, (c) aggregated colloid + AZ (10^{-5} M), (d) = (b) − (a)] and (II) the SH colloid [(e) nonaggregated colloid, (f) aggregated colloid with KNO_3, (g) aggregated colloid + AZ (10^{-5} M), (h) = (f) − (e)].

much higher morphological heterogeneity, since it is integrated by nanoparticles with a large spectrum of sizes and shapes. This correlates with the broader plasmon resonance extinction band, demonstrating the existence of small particles (indicated with arrows in Figure 3a), related to a slightly higher absorbance in the left part of the plasmon absorbance band due to the presence of small Ag clusters,[31] and rods and aggregates responsible for the higher absorbance at longer wavelengths. In contrast, the SH colloid shows spherical or quasi-spherical nanoparticles with a lower size dispersion. Even so, some clusters can be observed probably due to the aggregation induced by the solvent evaporation in the immobilization process.

Aggregated Ag Colloids. The addition of KNO_3 to an SC colloid preparation (Figure 4, panel I) induces a slight absorbance decrease of 0.05 absorbance unit (Figure 4b) in the plasmon resonance maximum of the nonaggregated SC colloid, which in this case appeared at 420 nm (Figure 4a). In addition, an increase of the absorbance is detected in the 600−950 nm region (inset). The difference spectrum (Figure 4d) reveals the existence of a band centered at ca. 700 nm corresponding to the formation of Ag aggregates. The addition of AZ to a previously activated SC colloid leads to a further absorbance decrease of 0.02 unit (Figure 4c). This behavior was observed in different SC batches.

In the case of the SH colloid, the addition of nitrate (Figure 4, panel II) induces a larger aggregation as shown in Figure 4f, with an absorbance decrease of 0.20 absorbance unit in the plasmon resonance of the nonaggregated SH colloid (Figure 4e), while the absorbance markedly increases in the 700−1100 nm region as can be seen in the difference spectrum (Figure 4h). The addition of AZ induced a strong aggregation of the colloid (Figure 4g). Therefore, the SH colloid is more sensitive to aggregation than the SC colloid.

The UV−vis absorption results of aggregated colloids are corroborated by the SEM micrographs (Figure 5), since global images of the immobilized SC (Figure 5a) and SH (Figure 5c) aggregates (registered with an amplification of only 2500×) show a higher aggregation extent in the case of the latter colloid.

The aggregates produced after the addition of AZ to SC (Figure 5b) and SH (Figure 5d) colloids are bigger than those induced by the addition of only nitrate, mainly in the case of the SH nanoparticles, in agreement also with the UV−vis spectrum. Besides, the SC and SH aggregates produced after aggregation with AZ display a markedly different morphology and fine structure as can be seen in Figure 6. While those aggregates formed with SC nanoparticles are smaller and much more compact (Figure 6a,b), the SH ones display a looser structure and a large amount of internal cavities (Figure 6c,d).

The different responses of SC and SH colloids to aggregation are related to chemical differences existing in the metallic surfaces. In fact, on the SC nanoparticles a higher ζ potential and thickness of the electrical bilayer (Stern layer) exist because of the higher negative electric charge provided by the citrate and its carboxylate oxidation products.[20] The lower potential existing on the SH nanoparticles explains why they are more easily aggregated by nitrate, AZ, or other adsorbates. Moreover, the existence of a high negative electric charge in SC nanoparticles may have an important influence on the nucleation and growing mechanism involved in the formation of these particles, being responsible for the final observed morphologies: small clusters, related to the difference absorption maxima observed at 348 and 374 nm, and rods. The formation of rods can take place through a chainlike growing mechanism involving a reaction-limited aggregation regime.[32] The situation is different in the SH nanoparticles, since the intermediate particles must be less stable and quickly aggregate to form spheroidal particles through a diffusion-limited aggregation regime.

Colloid Immobilization: Adherence on Glass. Figure 7 shows different SEM micrographs obtained for directly immobilized SC and SH colloids aggregated with nitrate on a glass cover slide. The SC aggregates lead to highly heterogeneous films by immobilization, where areas with a poor nanoparticle density and regions with a high concentration of nanoparticles (Figure 7a) and also areas of thick Ag films (Figure 7b) can be seen. In contrast, the immobilization of SH aggregates leads to a homogeneous distribution throughout the exposed glass surface (Figure 7c). This result suggests that SH nanoparticles have a higher adherence on the assayed glass surface. This effect is related to the existence of nitrogen oxides adsorbed on the SH nanoparticles. In fact, nitrogen oxides could react with silanol groups existing on the glass surface, inducing the protonation of these groups. Tsyganenko et al.[33] have demonstrated that the acidic properties of silanol groups existing on a glass surface can be enhanced in the presence of nitrogen dioxide. In this way, an ionic interaction of a positively charged glass surface and the SH nanoparticles with a negative charge in their surface could be induced.

SERS Spectroscopy. *Raman Spectra of the Colloids in the Absence of Analyte*. Figure 8 shows the macro-SERS

(31) Henglein, A. *Ber. Bunsen-Ges. Phys. Chem.* **1995**, *99*, 903.

(32) Weitz, D. A.; Lin, M. Y. *Phys. Rev. Lett.* **1986**, *57*, 2037.

(33) Tsyganenko, A. A.; Storozhev, E. N.; Manoilova, O. V.; Lesage, T.; Daturi, M.; Lavalley, J.-C. *Catal. Lett.* **2000**, *70*, 159.

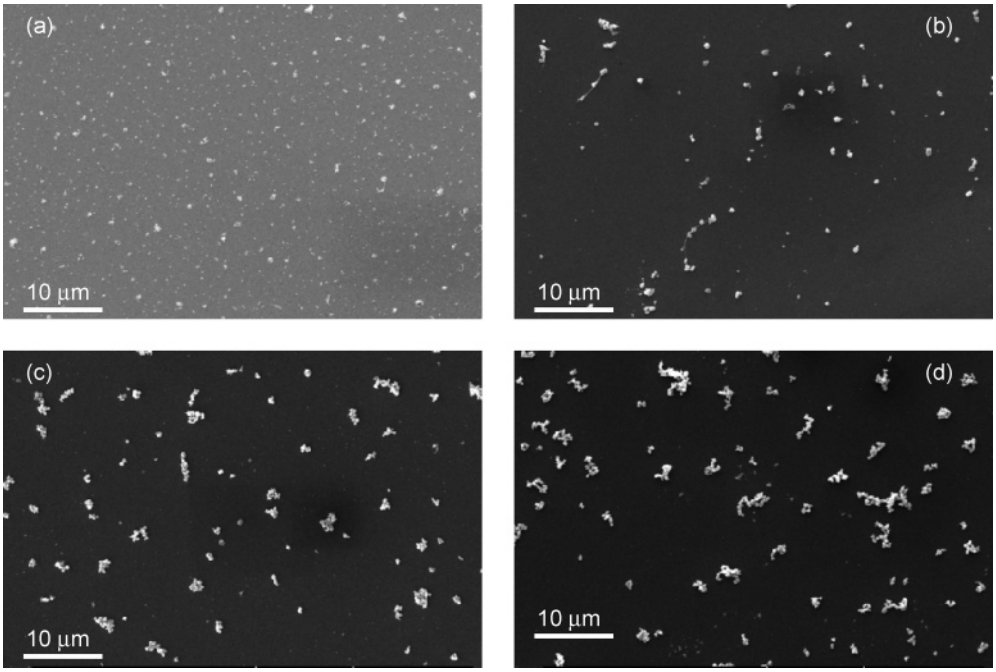

Figure 5. SEM micrographs of the SC colloid aggregated with KNO_3 (a) and KNO_3 + AZ(10^{-5} M) (b) and SEM micrographs of the SH colloid aggregated with KNO_3 (c) and KNO_3 + AZ (10^{-5} M) (d).

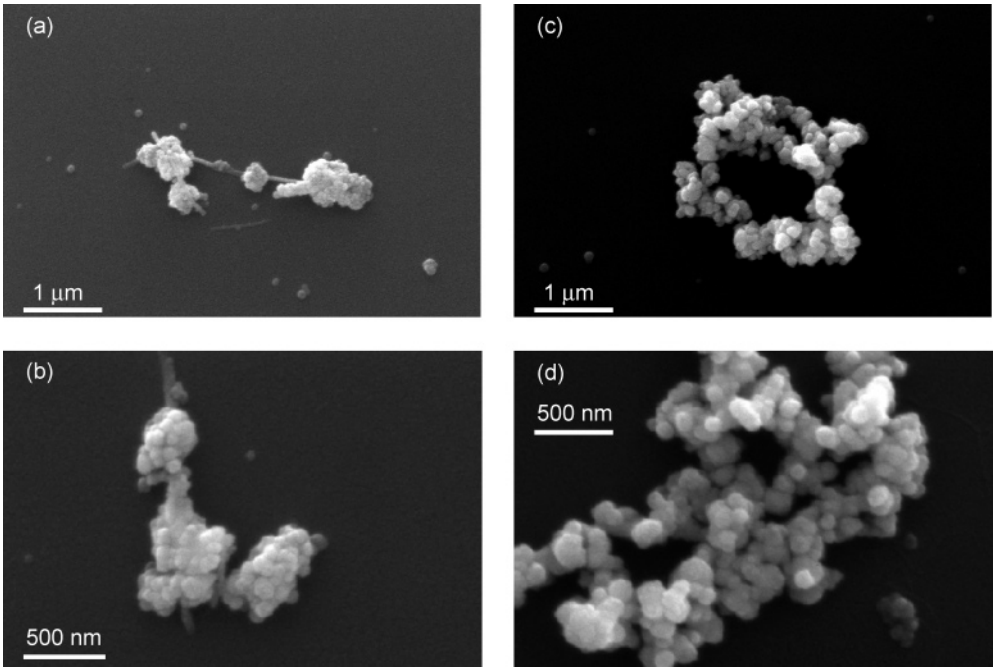

Figure 6. Detailed SEM micrographs of selected aggregates of SC (a, b) and SH (c, d) colloids obtained after aggregation with KNO_3 + AZ (10^{-5} M).

spectra of aggregated SC and SH colloids in the absence of AZ at different excitation wavelengths and after washing with water. The SC colloid (Figure 8a,b) displays a group of bands in the 1100−700 and 1300−1400 cm^{-1} regions (see Figure 8e for a more detailed representation of these regions) due to the citrate, as demonstrated by comparison with the Raman spectrum of citrate in aqueous solution (Figure 8f). These bands appear when excitation is done in the red or near-IR regions but are not seen at lower wavelengths. Besides, a band at 238 cm^{-1} is also observed attributed to the ionic species adsorbed onto the metal surface. However, the SH Raman spectra (Figure 8c,d) only show a narrow and intense band at 244 cm^{-1} attributed to the ν(Ag−Cl) vibration and a weaker band at 160 cm^{-1} which is attributed to the existence of Ag clusters on the metal nanoparticles due to the action of chloride.[34]

Figure 9 shows the micro-SERS spectra registered from different immobilized SC (panel I) and SH (panel II) nanoaggregates on a cover glass corresponding to the same sample used to obtain the micrographs in Figure 5a,c. In the case of the SC colloid a high variation in the Raman spectra was found from aggregate to aggregate. In some cases many features in the 1130−800 and 1400−1250 cm^{-1} regions appear (Figure 9b−d), which

(34) Sanchez-Cortes, S; Garcia-Ramos, J. V. *Surf. Sci.* **2001**, *473*, 133.

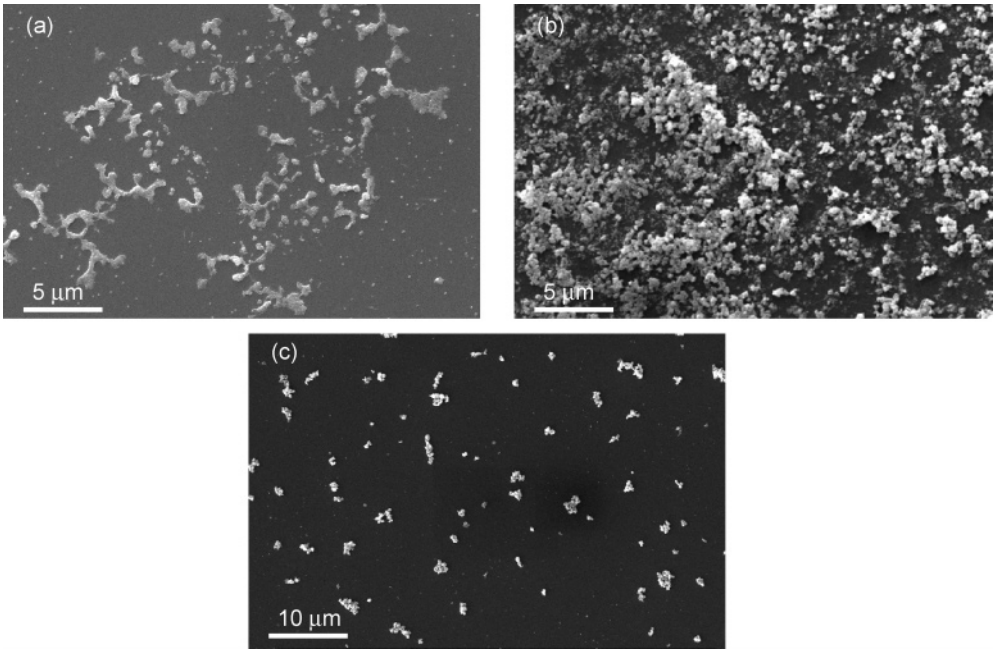

Figure 7. SEM micrographs of selected areas corresponding to the immobilization of SC (a, b) and SH (c) colloids on glass after aggregation with KNO_3 to view the immobilization patern of each kind of nanoparticle.

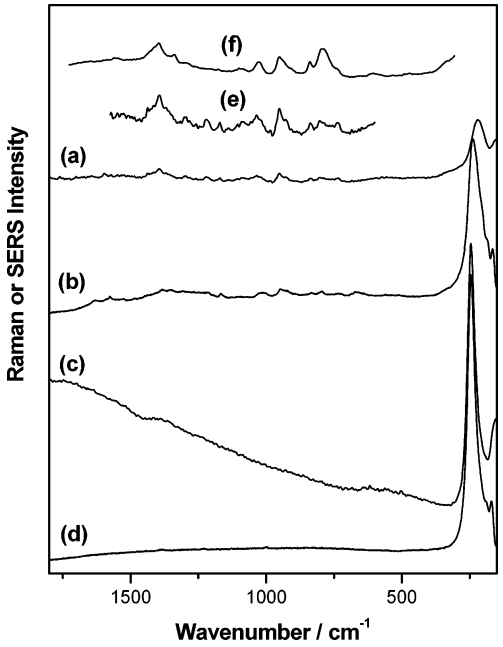

Figure 8. Macro-SERS spectra of SC (a, b) and SH (c, d) colloids after aggregation with KNO_3 with excitation at 1064 (a, c) and 785 (b, d) nm. Spectrum e corresponds to spectrum a multiplied by a factor of 3. Spectrum f is the Raman spectrum of potassium citrate in an aqueous solution, 0.1 M.

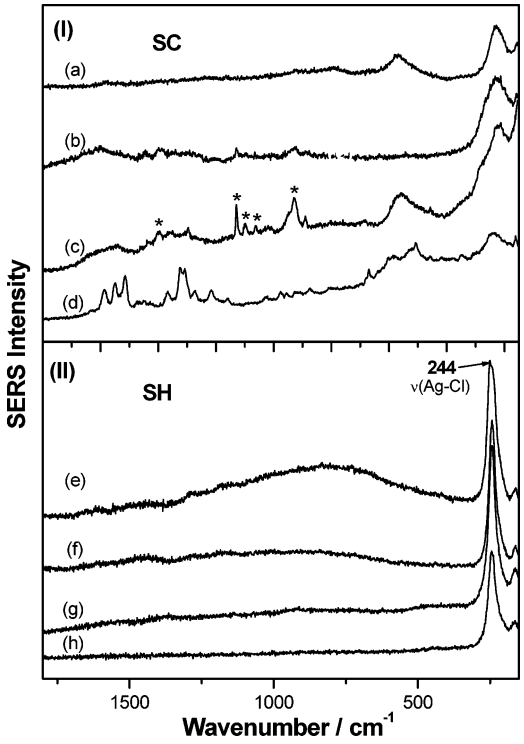

Figure 9. Micro-SERS spectra of SC (a−d) and SH (e−h) immobilized aggregates obtained after aggregation with KNO_3. The different spectra correspond to different analyzed aggregates.

may change with time. These features could correspond to impurities naturally occurring on the particle surface or to photodegradation products of the chemical species existing in the sample, especially to degradation products of citrate, as they are substantially different in comparison to the citrate bands appearing in macro-conditions (Figure 8e). Recently, Monti et al.[35] have reported that a variable spurious single-aggregate spectrum can be produced by nanoparticle luminescence. However, the fact that no spurious bands are observed in the case of SH nanoparticles (Figure 8e−h), where only an intense ν(Ag−Cl) vibration is observed at 244 cm^{-1}, indicates that the spurious bands observed in the case of SC nanoparticles are rather attributed to the chemical decomposition of citrate occurring on the metal surface upon laser irradiation as was also proposed by Bjerneld et al.[36]

(35) Monti, O. L.; Fourkas J. T.; Nesbitt, D. J. *J. Phys. Chem. B* **2004**, *108*, 1604.

(36) Bjerneld, E. J.; Xu, H.; Käll, M. In *Proceeding of the XVIIIth International Conference on the Raman Spectroscopy (ICORS)*; Mink, J., Jalzovszky, G., Keresztury, G., Eds.; John Wiley & Sons Ltd.: Chichester, U.D., 2002; p 269.

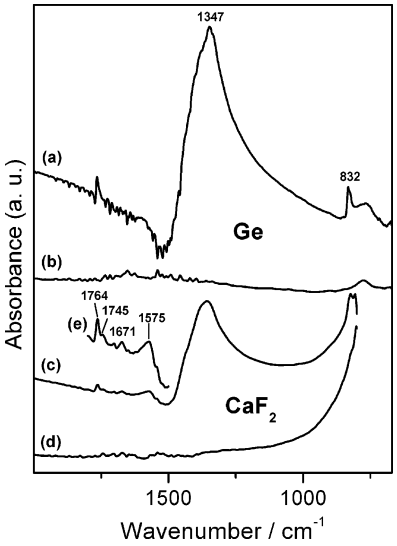

Figure 10. SEIR spectra of immobilized SH nanoparticles on Ge before (a) and after (b) washing with tridistilled water. SEIR spectra of SC nanoparticles on CaF_2 before (c) and after (d) washing with tridistilled water. Spectrum e is spectrum c expanded in the 1800−1500 cm^{-1} region.

Therefore, even after the immobilized colloids are washed, residues of citrate (and its oxidation products) as well as chloride still remain in the Ag nanoparticles.

SEIR Spectra of Immobilized Colloids in the Absence of Analyte. The SEIR spectra of SC and SH nanoparticles immobilized on CaF_2 before and after washing with water are displayed in Figure 10. The presence of nitrate is revealed by a strong band at 1347 cm^{-1} and another weaker band at 832 cm^{-1}, which completely disappear after washing with water (Figure 10b,d). Moreover, in the SEIR of SC nanoparticles (Figure 10c) weak bands can be seen between 1764 and 1575 cm^{-1} which could be attributed to the citrate and its oxidation products.[37,38] The bands at 1745 and 1671 cm^{-1} (Figure 10e) can be attributed to ν(C═O) of carboxylic acids and ketones, while the band at 1575 cm^{-1} is attributed to $\nu_{as}(COO^-)$ carboxylate anions.[37,38] However, the band at 1764 cm^{-1} is also present in the SEIR of SH nanoparticles and could be due to the existence of a common species in both colloids. According to the SEIR spectra, all these bands disappear after washing with water, but the SERS spectra demonstrate that small amounts of these ions still remain after washing.

SERS Activity of Ag Colloids in the Presence of AZ. Figure 11 shows the macro-SERS spectra of AZ on SC and SH colloids studied at two different excitation wavelengths (1064 and 785 nm). The SERS intensity of the AZ spectrum on SH colloids (Figure 11b) is higher than on SC colloids (Figure 11a) when the line at 1064 nm is used. This can be explained on the basis of the results obtained using UV−vis spectroscopy (Figure 4): the absorption band of SH nanoaggregates is much more intense in the near-IR region than that of the SC colloid. However, at 785 nm the SERS intensity on the SC colloid (Figure 11d) is higher than on the SH colloid (Figure 11e), which is related to the absorption maximum at 700 nm in the SC colloid. Therefore, this result demonstrates that even if SC and SH colloids display similar plasmon resonance profiles, their different responses toward aggregation extremely condition their SERS activity.

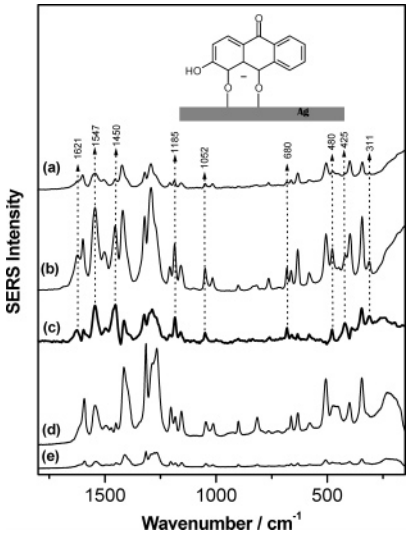

Figure 11. Macro-SERS spectra of AZ (10^{-5} M) on SC (a, d) and SH (b, e) colloids after aggregation with KNO_3 with excitation at 1064 (a, b) and 785 (d, e) nm. Spectrum c corresponds to the difference between spectra b and a.

As concerns the spectral profile, the SERS spectra obtained on each colloid show significant changes which are more clearly displayed in the difference spectrum of Figure 11c. The positive bands correspond to those features which increased their intensity in the SH colloid, which were assigned to monoionized AZ^- species.[27] This species interacts with the metal surface through the keto and hydroxyl groups existing in positions 9 and 1, respectively, as indicated in the inset of Figure 11. As these bands are more intense at lower pH values, we suggest that even if the macroscopic pH of both colloids is the same (6.5), there could be slight changes in the pH of the microenvironment surrounding the metal nanoparticles which may induce changes in the adsorbate protonation. These difference bands are less intense when excitation is done at 785 nm due to a resonant mechanism. Furthermore, the SC colloid has the disadvantage of the interference bands that can be seen in the SERS spectra, mainly at low concentration of the dye (result not shown). In the case of the SH colloid, these bands do not appear.

Conclusions

The physicochemical properties of Ag nanoparticles prepared by chemical reduction are strongly determined by the nature of the used chemical reductor. In particular, Ag nanoparticles prepared by reduction with citrate and hydroxylamine show significant differences in physical (morphology, plasmon resonance) and chemical (aggregation, adherence on glass, adsorption of molecular species) surface properties. The surface properties of nanoparticles are determined by the anions adsorbed on the nanoparticles, which stabilize them, preventing colloid flocculation. On the other hand, the presence of these anions may also influence the nucleation and growing processes occurring during the nanoparticle nucleation, which are responsible for the final nanoparticle morphology. The presence of citrate in SC nanoparticles induces the formation of small particles due to the high superficial negative electric charge as well as the formation of a large amount of rods, which are characteristic of these kinds of colloids.

The comparative study of the SC colloid versus the SH colloid reveals that the latter is more easily aggregated, showing a higher tendency to be immobilized on a glass surface, as revealed by the homogeneity of its immobilized

(37) Floate, S.; Hosseini, M.; Arshadi, M. R.; Ritson, D.; Young, K. L.; Nichlos, R. J. *J. Electroanal. Chem.* **2003**, *542*, 67.

(38) Nichols, R. J.; Burgess, I.; Young, K. L.; Zamlynny, V.; Lipkowski, J. *J. Electroanal. Chem.* **2004**, *563*, 33.

films. As concerns the application of these colloids to SERS and SEIR, both SC and SH colloids display impurity SERS bands even after the immobilized particles are washed, which cannot be detected by IR. However, the SH colloid does not show interference bands in important regions of the Raman spectrum. In micro-SERS experiments, no fluctuations were observed when using the SH colloid in comparison to the SC colloid, which displays a broad variety of interference bands attributed to thermal degradation of citrate and/or its products.

The SERS enhancement factor of each colloid depends on the plasmon resonance induced by the aggregation at a certain excitation wavelength, while the spectral profiles of the molecules exposed to the metal surfaces may change due to the different physicochemical surface properties of the SC and SH nanoparticles.

In conclusion, the results reported in this work demonstrate that the choice of Ag colloid preparation method for SERS measurements is strongly dependent on the experimental setup employed: macro- versus micro-SERS sampling, suspension or immobilized nanoparticles, aggregation degree of the final aggregates, excitation wavelength, and the chemical nature of the molecule under study. These findings can be very useful to researchers who work on Ag nanostructures and who are interested in the application of these systems to study the Raman spectra of organic molecules.

Acknowledgment. This work was supported by Dirección General de Investigación (Ministerio de Educación y Ciencia) Project Number FIS2004-00108 and Comunidad Autonoma de Madrid Project Number GR/MAT/0439/2004. This work also received support from the Red Temática de Patrimonio Histórico y Cultural (CSIC). M.V.C. acknowledges CSIC for an I3P fellowship founded by the European Social Fund.

LA050030L